BABES-BOLYAI UNIVERSITY, CLUJ-NAPOCA
BUDAPEST UNIVERSITY OF TECHNOLOGY AND ECONOMICS

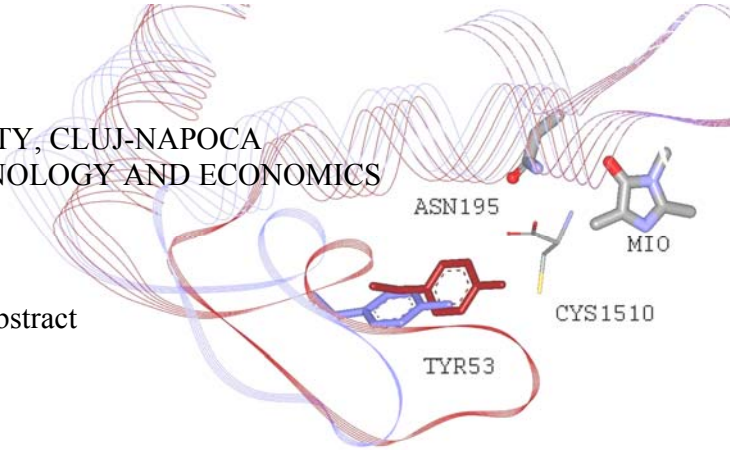

Ph. D. Thesis Abstract

Seff Amalia-Laura

ANALYSIS OF ENZYME-CATALYZED REACTIONS BY COMPUTATION

Scientific Advisers:
Prof. Dr. Ioan Silaghi-Dumitrescu†
Prof. Dr. László Poppe
Acad. Prof. Dr. Ionel Haiduc

Jury

President
Conf. Dr. Cornelia Majdik

Reviewers:
Prof. Dr. Paul Mezey, Memorial University of Newfoundland. Canada
CR1 (CNRS) Dr. Dragoş Horvath, University of Louis Pasteur Strasbourg, France
Conf. Dr. Radu Silaghi-Dumitrescu, Babes-Bolyai University, Cluj-Napoca

Public Defense:
July, 9th 2010
Cluj-Napoca

Table of Contents

Abbreviations

1B8F$_{mod}$	Partially modified structure of the histidine ammonia-lyase (1B8F)
1GKM$_{mod}$	Partially modified structure of the L-cysteine inhibited histidine ammonia-lyase (1GKM)
1W27$_{mod}$	Partially modified structure of the phenylalanine ammonia-lyase (1W27)
B3LYP	Becke's three parameter hybrid functional combined with the Lee-Yang-Parr correlation functional
CS	Systematic conformational search
DFT	Density functional theory
E_1cB	ammonia elimination mechanism by Michael addition
EC	Enzyme Commission number system
FC	Friedel-Crafts type mechanism
HAL	histidine ammonia-lyase
MIO	3,5-dihidro-5-metilidén-4*H*-imidazol-4-on group
MM	Molecular mechanics
N-MIO	Covalent intermediate of the HAL reaction bound to MIO *via* the amino group of L-histidine
PAL	phenylalanine ammonia-lyase
PDB	Brookhaven Protein Data Bank
PI	2-aminoindane phosphonate inhibitor
TAL	tyrosine ammonia-lyase
TAM	Tyrosine-2,3-aminomutase
QM	Quantum mechanics method
QM/QM	hybrid quantum mechanical methods

Keywords: phenylalanine ammonia-lyase • histidine ammonia-lyase • homology modeling • conformational analysis • docking • DFT • Zn^{2+}

Introduction

Investigation of the mechanisms of enzyme-catalyzed reactions by computational modeling has advanced significantly in the last years. Computer modeling methods can investigate some important questions about enzyme mechanism and catalysis that cannot be easily studied by experiment.

The PAL, HAL and TAL enzymes catalyze the elimination of ammonia from L-phenylalanine, L-histidine and from L-tyrosine when (*E*)-cinnamic, (*E*)-urocanic and (*E*)-coumaric acids are formed. These ammonia-lyases require the presence of the MIO electrophilic prosthetic group. The crystal structures found for PAL and HAL have the mechanistically significant Tyr loop region out/missing (PAL, PDB code: 1W27/1T6P) or as a partially opened (HAL) conformation in which the mechanism of the reaction could not be investigated by computation.

It was observed that a number of different metal ions, like Cd^{2+}, Mn^{2+} or Zn^{2+}, can increase the activity of the HAL enzyme. This experimental information was the reason why during this research we analyzed the active center of the partially modified crystal structure of HAL in presence of a Zn^{2+} ion.

During this Ph.D. research, we wanted to verify the following aspects included in the analysis of the mechanism of reactions catalyzed by ammonia-lyases using different computational tools:

- the first step was to construct *in silico* partially modified PAL and HAL structures starting from related known crystal structures where the active centers are totally closed and compact;
- a systematic conformational analysis of the covalently bound substrate to the MIO group in the active centers of the partially modified crystal structures was another part of this research;
- determination of the possible geometrical orientation of substrates and products within the closed active center of PAL/HAL using geometry optimization and ligand docking;
- calculation of the Th/Tbp complexation mode of Zn^{2+} in the presence of the substrate L-histidine within the closed conformation of the active site of HAL;
- determination of the acidity of *pro-(S)* β-hydrogen from L-histidine, L-4nitro-histidine and from Zn^{2+} complex through calculations at density functional theory (DFT) level. Here the zinc ion could affect the acidity of the *pro-(S)* β-hydrogen, allowing it to be abstracted by a base more easily.

1. Literature data

1.1. Ammonia-lyases

1.1.1 Ammonia-lyase structures

Because PAL, HAL and TAL catalyze almost the same reaction (in which elimination of ammonia happens from amino acids with aromatic rings forming α,β – unsaturated acids), these enzymes are similar in their structures. The similarity between the crystal structures is shown in Figure **1A**, **B**, **C** and **D**, and Figure **2A**, **B** and **C**).

HAL, PAL and TAL contain 4 active sites in the own homotetramer. Every monomer from the enzyme structure has an inner and an outer loop in the important Tyr region. Each inner loop from the monomers is in the same region with the outer loop from the next monomer which has the opposite direction.

The published[1] crystal structure of tyrosine ammonia-lyase – (wild type *Rhodobacter sphaeroides*, PDB code: 2O7B, Figure **1D**) – has a more closed and compact conformation of the interested loop region (Figure **1H**), as in case of the crystal structure found for bacterial HAL enzyme (*Pseudomonas putida*, PDB code: 1B8F, Figure **1A**)[2], where the inner loop from the active center (Figure **1E**) is not fully closed and we cannot identify an outer loop part. In case of *parsley* PAL X-ray structure[3] (*Petroselinum crispum*, PDB code: 1W27, Figure **3C**), the conformation of the significant Y110 loop region from the active site (Figure **1G, 2A**) is opened and inactive, in comparison with the X-ray structure[4] of *yeast* PAL (*Rhodosporidium toruloides*, PDB code: 1T6P, Figure **1B**), where the catalytically essential Y110 loop region (from Q104 to T122 sequence in the inner part and H345 to R359 in the outer loop) is missing (Figure **1F**).

The bacterial *Pp*HAL (PDB code: 1GKM) structure[5] reveals a partially opened, solvent accessible active site (Figure **2B**). All the six crystal structures determined for HAL so far contain the catalytically essential Tyr53 in a partially open loop conformation. This may be the reason why these structures could not retain substrate or product related ligands. Only the 1GKM crystal structure of HAL (inhibited with L-cysteine) was determined in the presence of an inhibitor in the active center.

The nonoxidative elimination of ammonia from the substrates, catalyzed by HAL, PAL and TAL requires the presence of 3,5-dihydro-5-methylidene-4*H*-imidazol-4-one (MIO)[6,7] electrophilic prosthetic group.

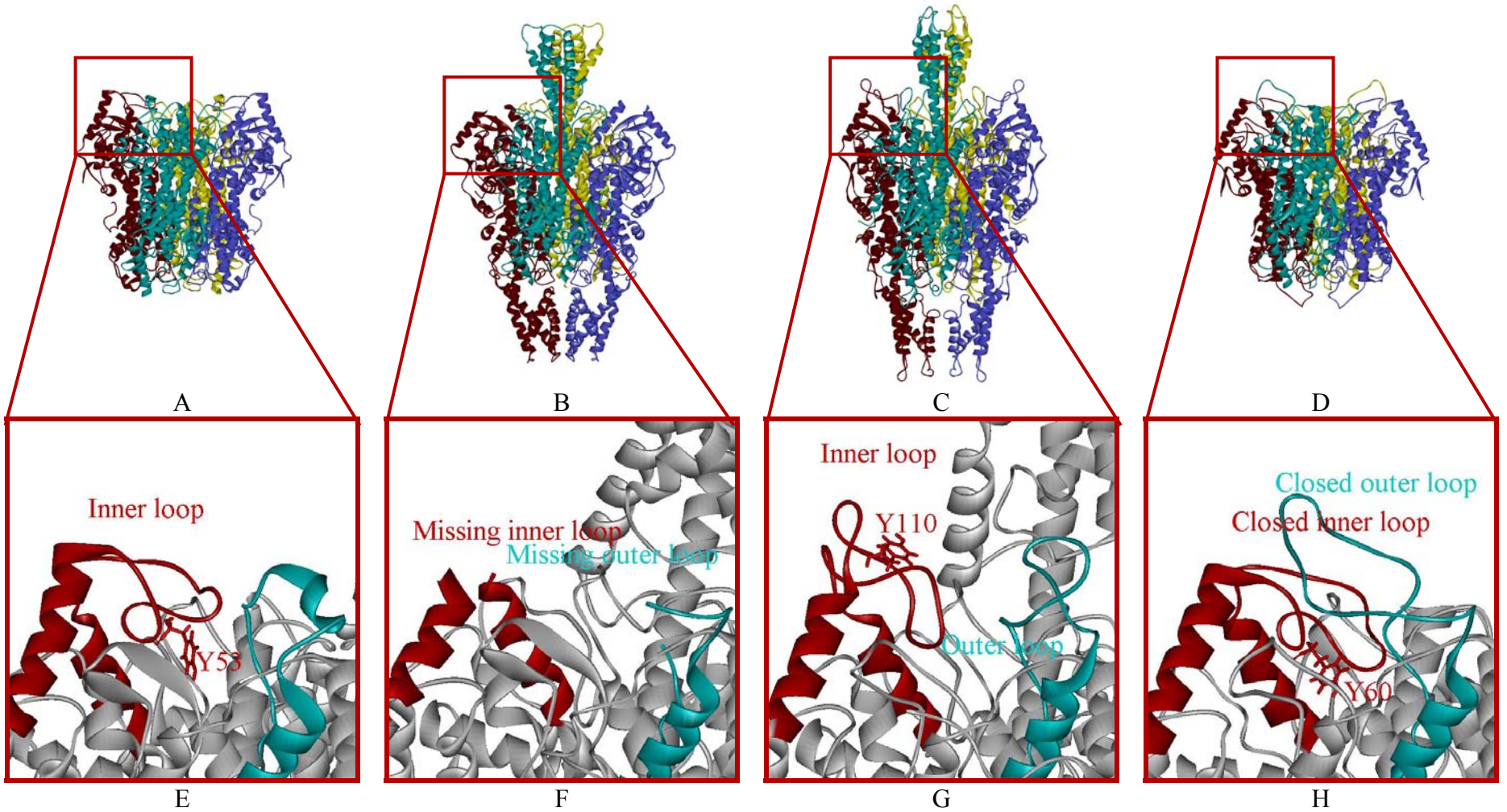

Figure 1. Ribbon representation of *Pp*HAL (PDB code 1B8F) homotetramer (A), *Rt*PAL (PDB code 1T6P) homotetramer (B), *Pc*PAL (PDB code 1W27) homotetramer (C) and *Rs*TAL (PDB code 2O7B) homotetramer (D) showing subunits A (yellow), B (violet), C (green) and D (red); Ribbon plot around the important Tyr amino acids (stick model) in (E) *Pp*HAL (PDB code 1B8F), (F) *Rt*PAL (PDB code 1T6P), (G) *Pc*PAL (PDB code 1W27) and (H) *Rs*TAL (PDB code 2O7B) crystal structures including a part of D (red) and C (green) chains.

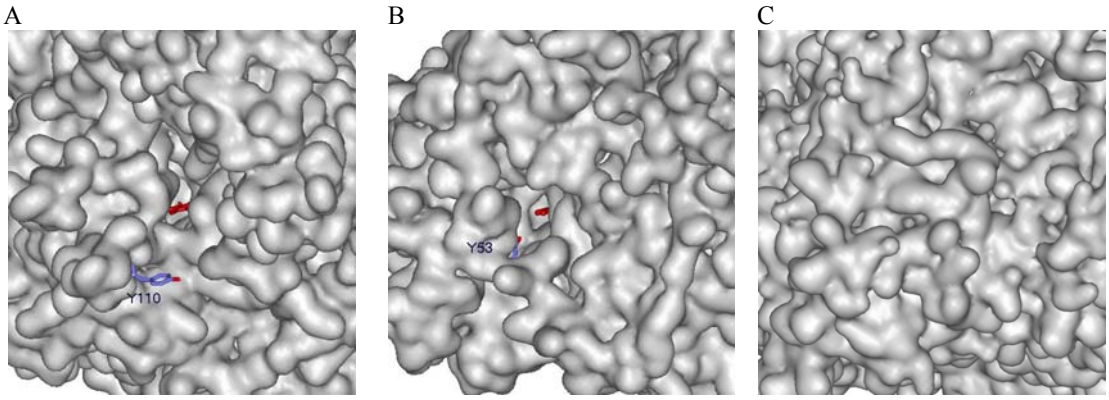

Figure 2. Comparison of the substrate entrance channel towards MIO group (red) in several ammonia-lyase structures. Representation of molecular surface of (A) *Pc*PAL (PDB code 1W27), (B) *Pp*HAL (PDB code 1GKM) and (C) *Av*PAL (PDB code 3CZO) crystal structures. The analogous Tyr110 (A) and Tyr53 (B) residues are seen as stick models in the partially opened ammonia-lyase structures.

The recently published ammonia-lyase crystal structure (PDB code: 3CZO),[8] determined for *Anabaena variabilis* PAL (*Av*PAL), contains the most compact active center in which the essential Tyr78 and the MIO prosthetic group are deeply buried and not solvent accessible (Figure **2C**).

1.1.2 Mechanism of PAL, HAL and TAL reactions

The MIO group similarity suggests that the HAL (EC 4.3.1.3), PAL (EC 4.3.1.24) and TAL (EC 4.1.3.23) behave similarly during the reaction of ammonia-lyases. HAL, PAL and TAL should remove the non-acidic *pro*-(*S*) β-proton from their substrates, without extracting the more acidic protons from the ammonium moiety of the corresponding L-amino acid. On the basis of the biochemical data two significantly different mechanisms were proposed for the reaction (Scheme **1**) of these ammonia-lyases.

According to Hanson and Havir,[9] the Michael addition (Scheme **1,** colored in red) of the amino group from the substrate to the MIO electrophilic prosthetic group of the enzyme takes place.

Typical for this mechanism is the formation of a covalent E-S intermediate (i.e. an *N*-MIO intermediate, Scheme **1**), where the amino group of the substrate is covalently bounded to the methylene part of the MIO prosthetic electrophilic group which facilitates the reaction owing to the formation of a better leaving group.[9,10]

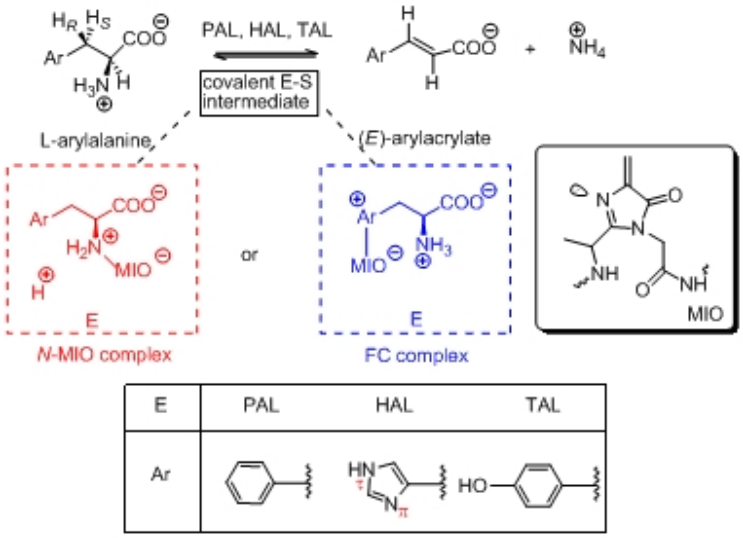

Scheme 1. MIO-containing ammonia-lyase catalyzed reactions. [The nitrogens in the imidazole ring of L-histidine and (*E*)-urocanate are denoted according to IUPAC with *pros* ("near", π) and *tele* ("far", τ)]

Due to the difficulty entailed by this possible mechanism to abstract the non-acidic *pro*-(*S*) β-proton by the enzymic base in the course of ammonia elimination, an alternative mechanism involving a Friedel-Crafts (FC) type attack at the aromatic ring of the substrates by the electrophilic prosthetic group has been suggested by Rétey.[11] This implies a σ-complex intermediate (Scheme **1**, colored in blue) between the aromatic ring and MIO.

ORIGINAL CONTRIBUTIONS

2. Models and methods

2.1. Homology modeling

The homology modeling method was used by us because we needed the closed form (catalytically active form) of the important Y-containing inner loop region of ammonia-lyase structures and the X-ray structures (PAL 1W27,[3] HAL 1B8F,[2] 1GKM[5]) of PAL and HAL were determined with an opened or partially opened active site (with a non-active conformation of the inner loop). The 1W27 determined for PAL, 1B8F and 1GKM crystal structures determined for HAL weren't able for computational investigation within the active site. Our aim was to modify only just a small amino acid sequence at the inner loop region which is in opened/partially opened form. For homology modeling, the Swiss-Model automated homology modeling service[12,13,14,15,16,17] was used. We took into account the amino acid sequence identity between the interested crystal structure and the template.

2.2. Conformational analysis within the rigid enzyme

2.2.1 Conformational analysis within the 1W27$_{mod}$ partially modified rigid parsley PAL structure

The initial ligand structure for systematic conformational search (CS) was built up from the 2-aminoindan-2-phosphonic acid inhibitor (PI) bound to MIO *via* its N-atom (from structure 2O7E).

In the 1W27$_{mod}$ PAL structure the PI ligand was introduced and for our study a 15 Å sphere around the MIO prosthetic group was cut off from the active site model. Next, by using HyperChem[18] standard procedure hydrogen atoms were added to the amino acid residues of this raw active site model. In this way the C- and N-termini at cutting were completed to neutral aldehyde and amino moieties. The MIO group was manually corrected.[18] During CS on the covalently bound phenylalanine and the heterocyclic ring of the MIO in rigid enzymatic environment (no water), 3 torsion angles of the ligand were varied for the *N*-MIO model. The conformational searches were performed by using the CS module[18] implemented in HyperChem

using default settings (MM+ forcefield; gradient: 0.1 kcal/mol; Polak-Ribiere method; limits: 300 iterations, 150 optimizations, 15 conformations; test options: "skip if atoms are closer than 0.3 Å").

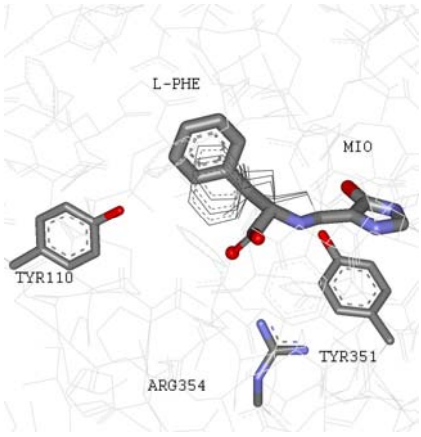

Figure 3. The conformational analysis results for the *N*-MIO intermediate of the natural substrate in PAL model. Tube model shows the best energy conformation of the *N*-MIO intermediate and the other conformations are depicted as wireframe model.

For each covalent intermediate model, the best ligand energy conformation was selected (Figure **3**) which was also in correspondence with the overall arrangement (aromatic moiety points towards Leu138 and carboxylate is in the close vicinity of Arg354) found in the experimental inhibited structures of TAL. The initial *N*-MIO active site model was built by replacing the PI-MIO part of the raw *Pc*PAL(1W27)/PI active site construct with the ligand arrangements resulted from the CS's.

2.2.2 2nd Type of conformational analysis for the covalently bound MIO-substrate intermediates within the partial 1GKM$_{mod}$ structure

Two separate CSs were performed for each covalently bound reaction intermediate [*N*-MIO, (*S,S*)-FC and (*R,S*)-FC models] bearing a proton on either the π or the τ nitrogen of the imidazole ring ($N_{\pi H}$ and $N_{\tau H}$ series of conformers). The six CS calculations involving the ligand and MIO [28 atoms in the *N*-MIO model and 29 atoms in the (*S,S*)-FC / (*R,S*)-FC) models] were performed in a rigid enzymic environment without water molecules. For the *N*–MIO model, three torsions [along the axes of $C_{(MIO\text{-}C5)}$–$C_{(MIO\text{-}CH2)}$, $C_{(MIO\text{-}CH2)}$–$N_{(HisL)}$, $N_{(HisL)}$–$C_{(HisL\text{-}C\alpha)}$], and for the (*S,S*)-FC and (*R,S*)-FC models four torsions [along the axes of $C_{(MIO\text{-}C5)}$–$C_{(MIO\text{-}CH2)}$, $C_{(MIO\text{-}CH2)}$–$C_{(HisL\text{-}C4)}$,

$C_{(HisL\text{-}C5)}$–$C_{(HisL\text{-}C\beta)}$ and $C_{(HisL\text{-}C\beta)}$–$C_{(HisL\text{-}C\alpha)}$] were varied during the CSs. The CSs were performed by the HyperChem implemented CS module[18] using the default settings (MM+ forcefield; gradient: 0.1 kcal/mol; Polak-Ribiere method; limits: 300 iterations, 150 optimizations, 15 conformations; test options: "skip if atoms are closer than 0.3 Å").

The resulted conformers of the covalent intermediates after systematic conformational search are presented in the Figure 4.

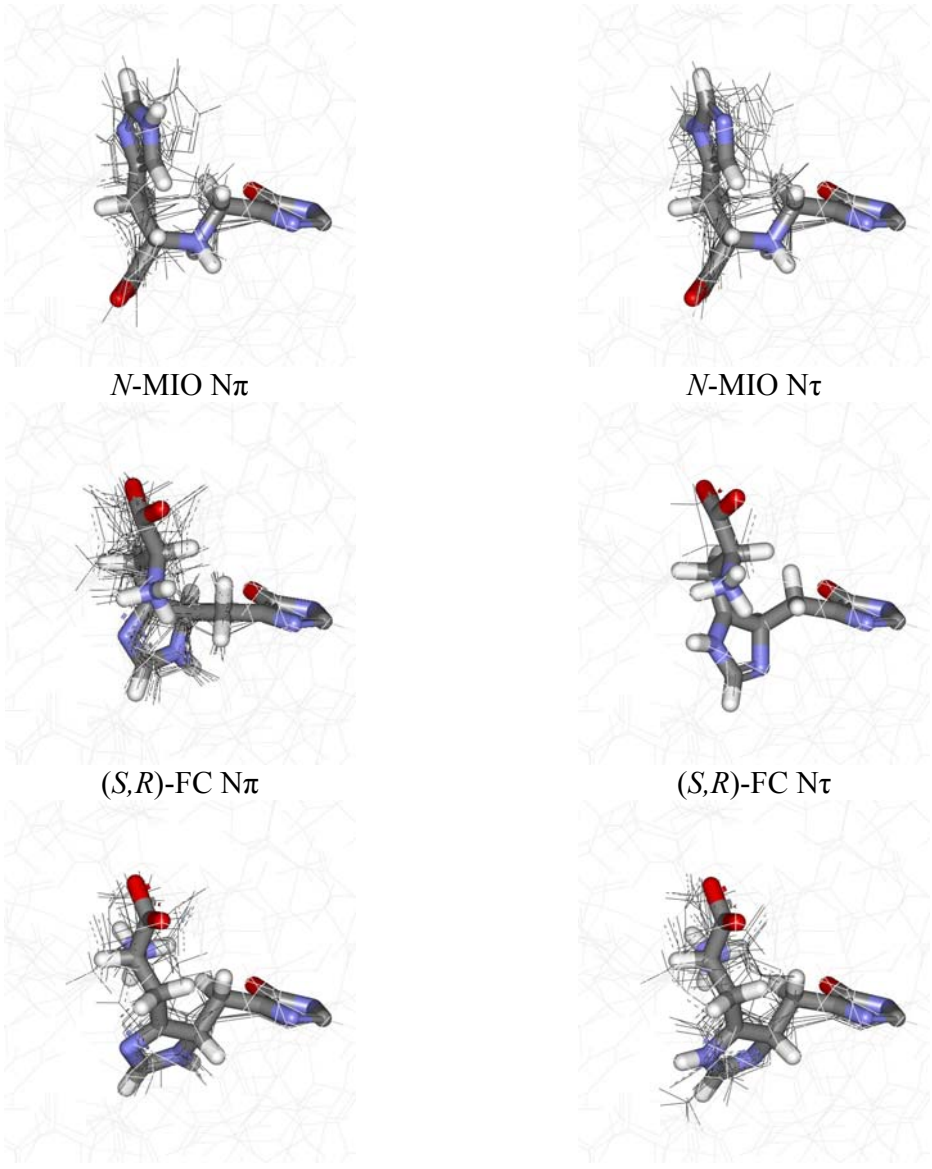

Figure 4. Results obtained after 2nd Systematic Conformational Search (CS) of the *N*-MIO, (*S,R*)-FC and (*S,S*)-FC covalent intermediates.

2.3. Geometry optimization of the covalent intermediates, L-histidine and (E)-urocanate within the active site of HAL

2.3.1 Geometry optimization after the 2nd type of conformational analysis

L-Histidine and (*E*)-urocanate structures were built, by proper rearrangement of bonds, from those conformers of the covalent intermediates which had straight main-chain conformation [*N*−MIO series ($N_{\tau H}$: c1-c3, c5, c8, c9, c11; $N_{\pi H}$: c1-c4, c6, c9, c10) Scheme **2**; (*R,S*)-FC series ($N_{\tau H}$: c2, c4, c5, c7-c9; $N_{\pi H}$: c2) and (*S,S*)-FC series ($N_{\tau H}$: c1-c2; $N_{\pi H}$: c2) Scheme **2**].

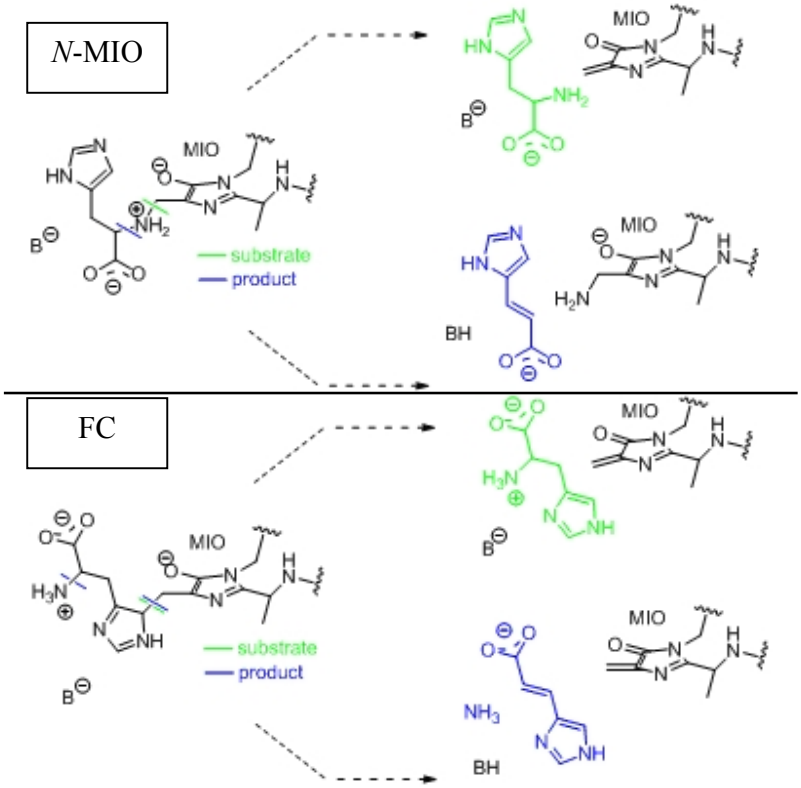

Scheme 2. Construction of the L-histidine (colored in green) and (*E*)-urocanate (colored in blue) containing active site models from the FC intermediate model of HAL.

In all substrate, intermediate and product structures, the ligand together with MIO (substrate, intermediate) or NH_2–MIO (product) and the His83, Tyr280, Tyr53, Asn195, Gln277, Glu414, Arg283 and Phe329 (a total of 116 atoms) were optimized in a 15 Å spherical part (2221 atoms) of the $1GKM_{mod}$ structure, while keeping the residual part rigid. The optimizations were performed by the HyperChem[18] implemented MM+ forcefield with the default settings (gradient: 0.1 kcal/mol; Polak-Ribiere method).

For the docking of different ligands within $1W27_{mod}$ PAL active site we used the Arguslab[19] software.

In case of $1GKM_{mod}$ for docking zwitterionic L-histidine, Tyr53 and Tyr280 were kept deprotonated and four torsion angles (along the axes of C_5-C_β, C_β-C_α, C_α-N and C_α-C_{COO}-) were varied, whereas for docking (*E*)-urocanate, protonated forms of Tyr53 and Tyr280 were used. Gasteiger charges were added to the atoms of the binding interfaces used for docking by AutoDock software.

2.4. DFT calculations on ligands involved in HAL reactions

DFT calculations were carried out on L-histidine and L-4-nitrohistidine models (both with protonated amino groups) for conformations corresponding to the HAL bound state, on a truncated model of the *N*−MIO-intermediate (by replacing the MIO ring of the calculated structure with a hydrogen atom at the exocyclic methylene carbon of MIO) and on a partial active site model including the truncated model of the *N*-MIO-intermediate in coordination with a Zn^{2+} ion, which is also coordinated to representative parts of His83 and Met382 and to a water. The DFT optimizations were performed using the GAUSSIAN 09 (rev. *A.1*)[20] and GaussView[21] as front-end. Two positively charged L-histidine structures (with –COOH and $-NH_3^+$) were constructed from the *N*−MIO models (from conformations c5 and c4 of the $N_{\tau H}$ and $N_{\pi H}$ series of CSs, respectively). Two positively charged L-nitrohistidine models were built from these two L-histidine structures by replacing the hydrogen at C_4 of the imidazole with a nitro group.

In the Zn^{2+} complex models, the Zn^{2+} ion had four or five ligands: the imidazole of the *N*–MIO ($N_{\pi H}$) ligand at the N_τ–atom (i.e. the c4 conformer of the *N*–MIO $N_{\pi H}$ series, with a $-NH_2(CH_3)^+$ group as a model of the amino moiety bound to MIO, truncated between the MIO ring and the exocyclic carbon), a 4-methyl-1*H*-imidazole (coordinated at N_τ, representing His83), a dimethyl sulfide (coordinated at its S-atom, representing Met382) and one (in the tetrahedral case) or two (in the trigonal bipyramidal case) water molecules. Proper constraints were used to maintain the conformation of the MIO-bound histidine ligand (HisL) as allowed within the HAL active site. For the Zn^{2+} complex models, several atomic positions were frozen [in Model 1: an oxygen atom of carboxylic acid moiety of the MIO-bound histidine ligand (the one which was closer to Arg283), the carbon atom of the methyl group of 4-methylimidazole (truncated His83); in Model 2: as in Model 1 + a carbon atom of the dimethyl sulfide (representing the C_γ atom of

Met382); in Model 3: as in Model 1 + methylene carbon atom of MIO; and in Model 4: as in Model 1 + a carbon atom of the dimethyl sulfide (representing the C_γ atom of Met382) and methylene carbon atom of MIO].

Full geometry optimizations for the two types of L-histidine, L-4-nitrohistidine and the tetrahedral or trigonal bipyramidal Zn^{2+} complexes were carried out by the DFT method using Becke's three parameter hybrid functional combined with the Lee-Yang-Parr correlation functional (B3LYP)[22,23] with the 6-31G or 6-31G(d,p) basis sets. After optimizations, vibrational frequencies were computed at the same level of theory and single point energies were calculated with a larger basis [6-311+G(d,p) for Zn^{2+}, for the two imidazole rings, for the $–S-CH_3$ part of Met382 and for the water molecule(s); and 6-31G(d) for the other parts of the Zn^{2+} complex models].

3. Results and discussion

3.1. The active ammonia-lyase structures

3.1.1 Modeling the active conformation of PAL

Based on HAL structures,[2] a modified parsley PAL structure was already built, which has a closer active center than the experimental PAL crystal structure.[8,24] Recently the TAL crystal structure was resolved,[1] in which the essential Tyr-containing loop region has a compact conformation and therefore has a more closed active site.

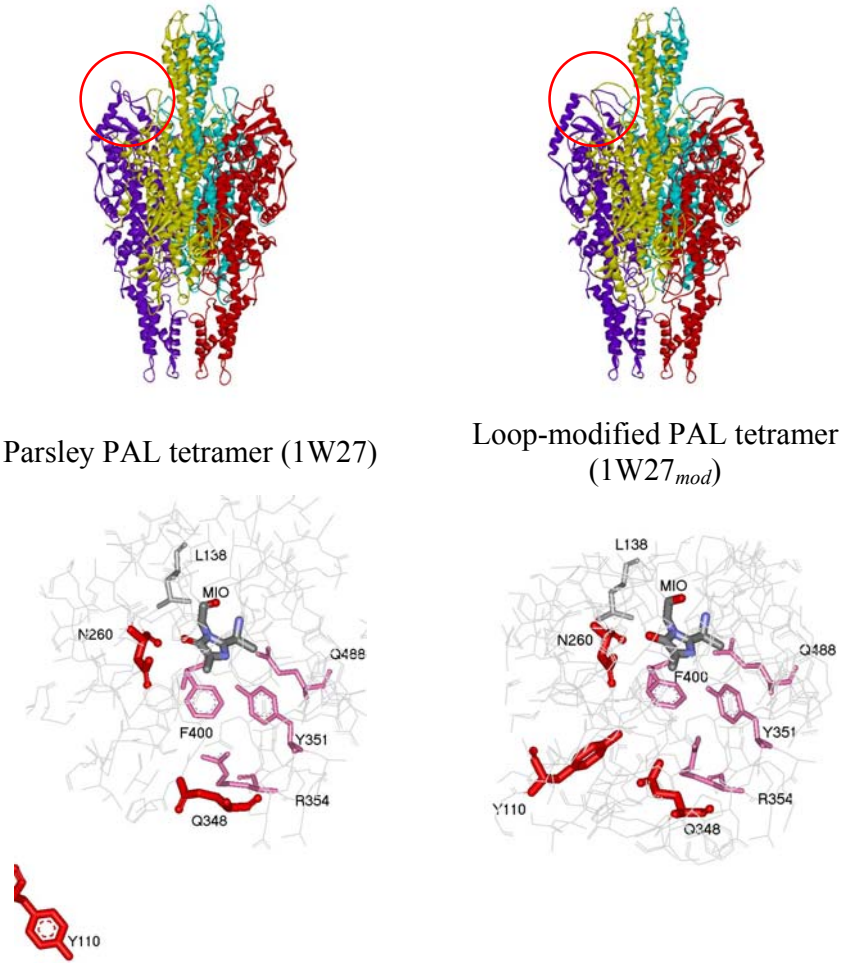

Figure 5. PAL tetramers and their active site

Based on the TAL (PDB code: 2O7B) structure,[1] a new loop-modified PAL model was built by us,[25] which has the important Tyr110 amino acid incorporated in the active site. The tetramers of the parsley PAL crystal structure and the PAL model can be seen in Figure 5. A

more detailed comparison of the two PAL active sites shows the Tyr110 residue in two different orientations.

Tyr110 in our model points in the direction of MIO, whereas in the crystal structure was far from the active site (Figure 5).

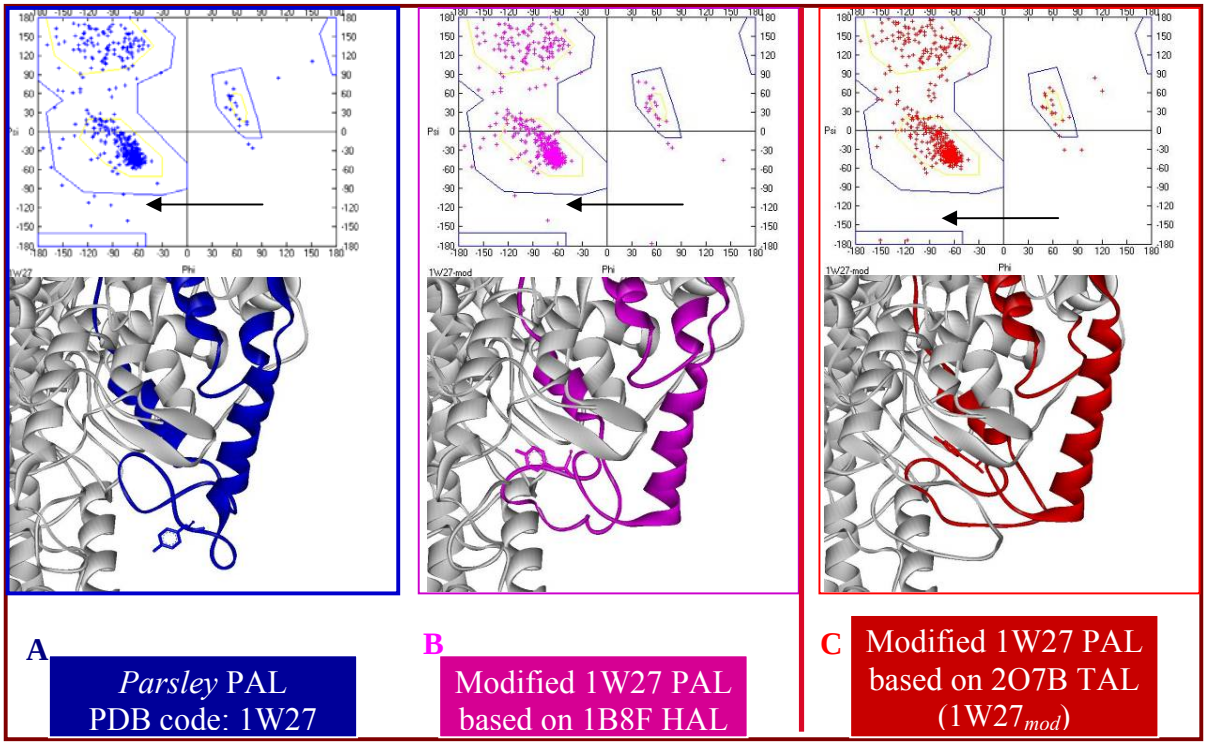

Figure 6. Presentation of experimental (1W27; blue), modified *P. crispum* PAL structures based on 1B8F HAL (pink) and on 2O7B TAL (red). The Ramachandran plot of the monomers are shown in every structure.

The partially modified *parsley* PAL structure ($1W27_{mod}$, Figure **6C**) has the most closed loop region and a compact active center.

After the construction of our TAL based model, a new X-ray structure of the *Anabaena variabilis* PAL enzyme (PDB code: 3CZO)[8] was published, in which the Tyr loop region essential for the reaction is the most closed and compact one from all of the crystal structures of ammonia-lyases. Analysis of our TAL-based model showed good match with the 3CZO structure in the Tyr loop region.

Notably, the Tyr110 in the TAL based $1W27_{mod}$ PAL model, C, is in an even better position than in case of B. This is because the TAL template is more compact in the Tyr loop region important for the reaction. *Ramachandran Plot* analysis of the monomers of experimental

parsley PAL (1W27), modified PAL based on 1B8F HAL and the $1W27_{mod}$ PAL indicated that from the 716 amino acid residues of a single subunit of the experimentally 1W27 structure 12 amino acids (six in the Y110 loop region), in the Y110 loop region of the 1B8F HAL-based modified 1W27 structure eight amino acids (only two in the Y110 loop region), but in the Y110 loop region of $1W27_{mod}$ structure only four amino acids (neither of them) are outside the likely Phi/Psi combinations (Figure **6**).

3.1.2 Modeling the active conformation of the HAL structures

3.1.2.1 Bacterial 1B8F *Pp*HAL structure with active conformation

Histidine ammonia-lyase (HAL, E.C. 4.3.1.3) is an important enzyme in the degradation of histidine in various bacteria.[26] In the first step of degradation of histidine the α-amino group elimination is catalyzed by HAL and the product is α-β-unsaturated *trans*-urocanate. Urocanate has been known as a sun blocker in human skin.[27] HAL absence in humans is known as a disease histidinemia.[28]

The crystal structure of bacterial HAL from *Pseudomonas putida* (PDB code 1B8F) determined at 2.1Å resolution reveal a partially open, solvent accessible (Figure **7B**) active site which contains the mechanistically relevant Y53 loop region (Figure **7A**). The active site in the recent crystal structure of TAL (PDB code 2O7B) is completely closed and not solvent accessible (Figure **7E**) in comparison with the active site of *parsley* PAL and *bacterial* HAL.

The important Tyr60 determined by direct mutagenesis is totally in the active site of TAL (Figure **7F**) in comparison with the position of Tyr53 from HAL (Figure **7C**).

For a better understanding of the reaction mechanism of ammonia-lyases, a closed active centre of HAL was necessary. Based on the homology model of 30-75 amino sequences of HAL on TAL X-ray structure (2O7B) we have built *in silico* a partially modified HAL crystal structure[29] with a completely closed active center (Figure **7G** and **7I**).

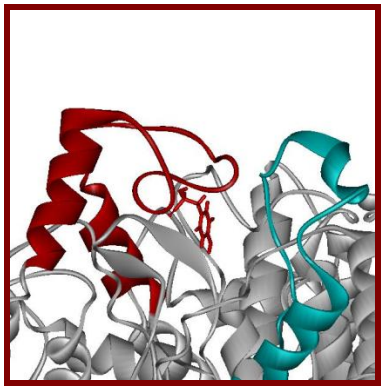

A) The essential Y53 loop region in HAL structure

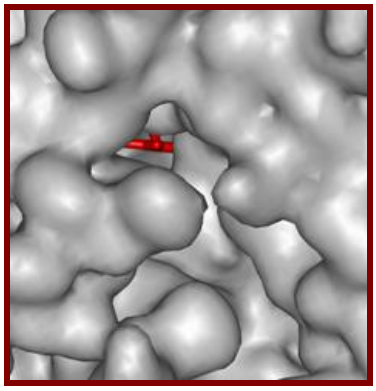

B) Molecular surface representation

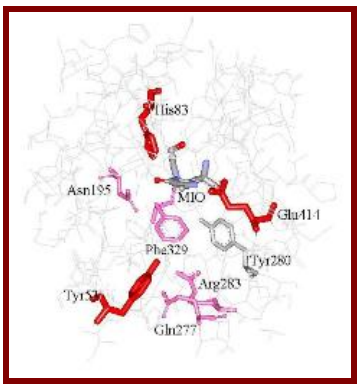

C) Active site amino acids of HAL enzyme

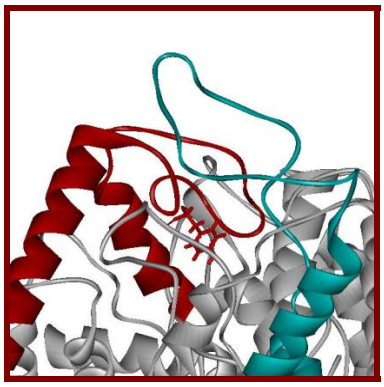

D) The essential Y60 loop region in TAL structure

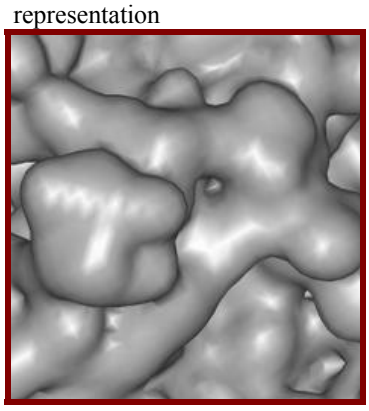

E) Molecular surface representation

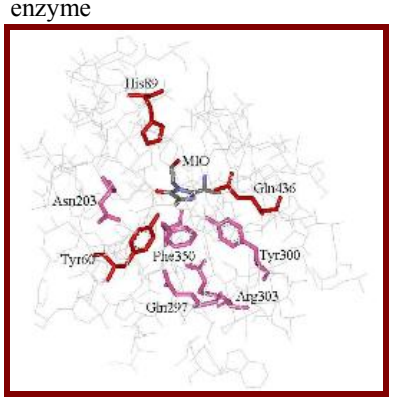

F) Active site amino acids of TAL enzyme

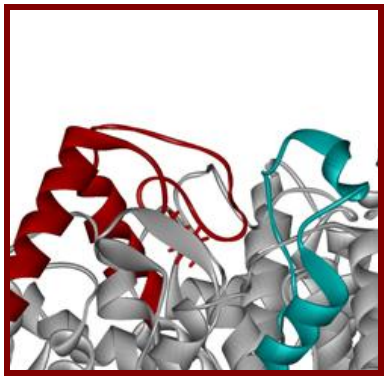

G) The essential Y53 loop region in 1B8F$_{mod}$ HAL

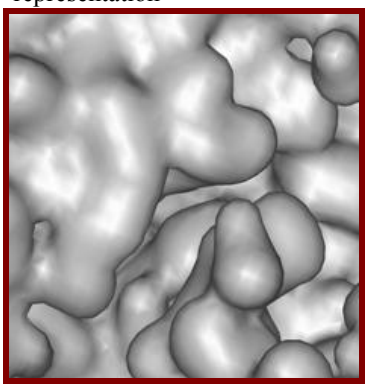

H) Molecular surface representation

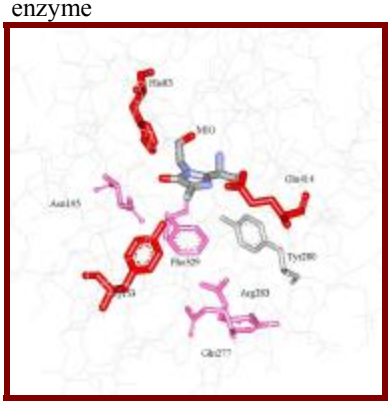

I) Active site amino acids of 1B8F$_{mod}$ HAL model

Figure 7. X-ray structures of *bacterial* HAL (1B8F), *bacterial* TAL (2O7B) and the partially modified HAL structure (1B8F$_{mod}$)

3.2. Computational investigation of the histidine ammonia-lyase: a modified loop conformation and the role of Zn (II) ion

3.2.1 Construction of a closed 1GKM HAL active site environment for calculations

The 1GKM is the only crystal structure of *Pp*HAL in which an inhibitor is present. Importantly, this is also the structure where the side chain of Met382 has a different conformation from the side chain arrangement of the other five unliganded *Pp*HAL structures.[2,30]

Although the existing six *Pp*HAL structures contain the Tyr53 inside the active site,[2,5,30] a structural comparison of HALs to the ammonia-lyases with tightly closed active sites indicated the Tyr-loops in all HAL structures are in a partially open conformation (Figure **8a**). The importance of the loop containing the catalytically essential tyrosine in the MIO-containing ammonia-lyases was best demonstrated for PAL. The Tyr-loops were missing[4,8,31] or were in catalytically inactive conformation[3,24] in several crystal structures of PAL. Only recently, the structure of PAL from *Anabaena variabilis* (*Av*PAL) containing a tightly closed active site confirmed the active conformation of the Tyr-loop.[8] Similarly, the crystal structure of *Rhodobacter sphaeroides* tyrosine ammonia-lyase (*Rs*TAL) revealed a tight active centre in which the loop containing the essential Tyr60 was present in active conformation.[1]

Comparison of the *Pp*HAL (1GKM, in blue) structure to *Rs*TAL (2O7B, in green)[1] and *Av*PAL (3CZO, in orange and CPK color)[8] with compact active centers revealed that the catalytically essential Tyr53-containing loop of *Pp*HAL adopts a partially open conformation (Figure **8a**). Because the most compact structure has been found for *Av*PAL (3CZO, 2.2 Å resolution) containing the non-solvent accessible essential Tyr78 and the electrophilic MIO deeply buried in the active center,[8] this ammonia-lyase structure has been selected as a template for modeling the compact conformation of the Tyr-loop of *Pp*HAL.

Comparison of the Tyr53 containing inner loop region of the modified *Pp*HAL (1GKM$_{mod}$, Figure **8b**, in red) to the Tyr-loop of the original L-cysteine inhibited *Pp*HAL (1GKM, Figure **8b**, in blue) indicated that the catalytically essential Tyr53 in the modified structure was closer to MIO, and therefore could better facilitate the *pro*-(*S*) β-proton elimination from the substrate, than in the original HAL structure. Moreover, Ramachandran-plot analysis of single subunits of the two HAL structures revealed that there were 8 amino acid residues outside the likely Phi/Psi combinations in the original HAL structure (1GKM, Figure **8c**), whereas there were only 4 unlikely combinations in the Tyr53-loop of the modified HAL structure (1GKM$_{mod}$, Figure **8d**).

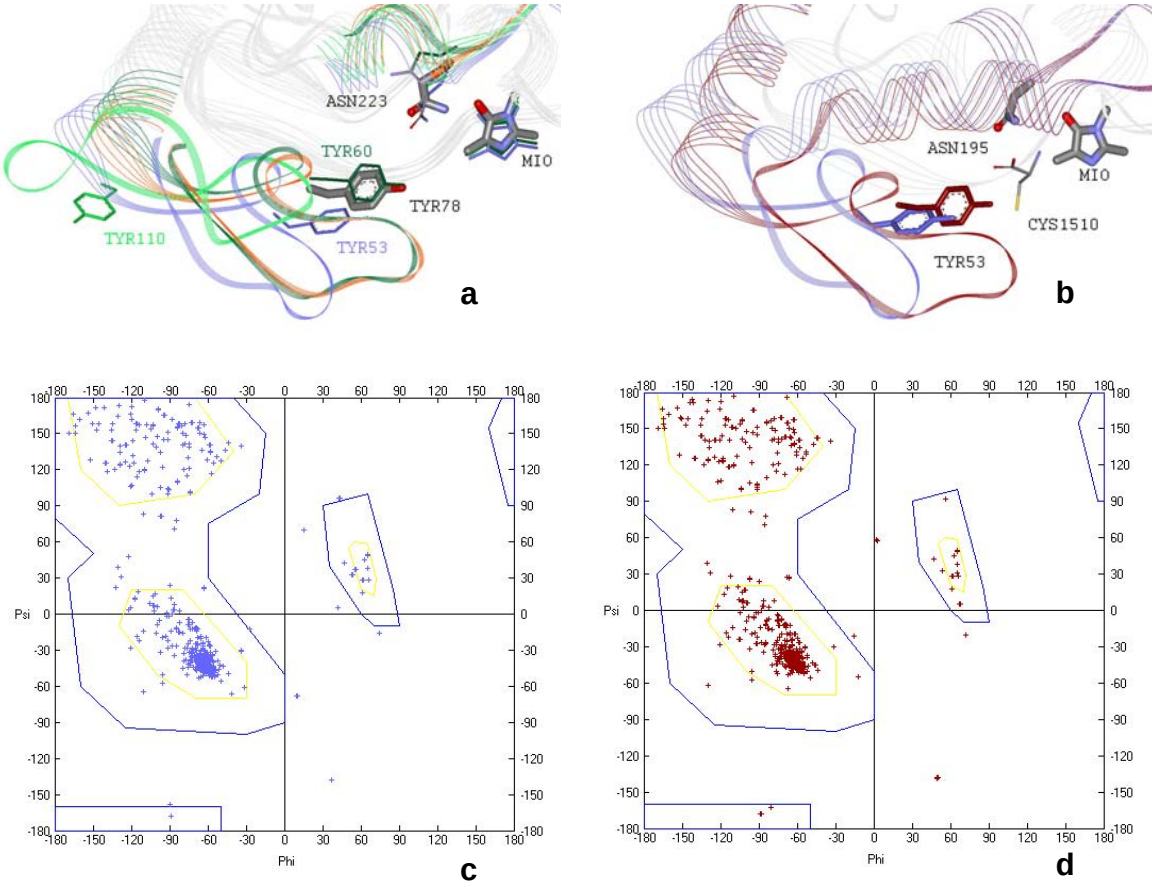

Figure 8. The mobile Tyr-loops in the active site of MIO-containing ammonia-lyases. **a.** Comparison of two mobile regions (including the MIO stabilizing Asn and the catalytically essential Tyr residues) of four different ammonia-lyases: *Anabaena variabilis* PAL (3CZO, in orange and CPK color); *Petroselinum crispum* PAL (1W27, in bright green); *Rhodobacter sphaeroides* TAL (2O7B, in dark green); *Pseudomonas putida* HAL (1GKM, in blue). The Asn residue is numbered according to *Av*PAL (3CZO). **b.** Overlay of the essential Tyr53 loop regions of *Pp*HAL (1GKM inhibited with L-cysteine, colored by CPK, blue chain) and the Tyr-loop modified *Pp*HAL (1GKM$_{mod}$, red chain). **c.** and **d.** Ramachandran plots for monomeric units of *Pp*HAL (1GKM) and the partially modified *Pp*HAL (1GKM$_{mod}$), respectively.

3.2.2 Comparison of the conformation of the covalent reaction intermediates of the HAL reaction with the arrangements of the substrate and product

Some early reports have indicated that treatment of HAL at high pH in the presence of L-cysteine and oxygen leads to an irreversible inactivation of the enzyme.[32,33] On denaturation, the L-cysteine inhibited HAL, followed by pronase digestion resulted in two main chromophoric products.[34] In one product, the exocyclic methylene of the MIO was substituted by the amino

groups of L-cysteine. When L-cysteine inhibited HAL was first digested with trypsin, two chromophoric 24-residue peptides were isolated and identified as *N*–MIO fragments.[35] This was later supported by the L-cysteine inhibited structure of *Pp*HAL (PDB code: 1GKM[5]). The inhibited HAL contains the inhibitor with its amino moiety close to the exocyclic methylene of the electrophilic MIO prosthetic group. This fact can be considered as a further proof for the presence of an amino-enzyme intermediate in the HAL reaction demonstrated by Peterkofsky.[36]

Structures of the HAL with L-cysteine,[5] TAL with 2-aminoindan-2-phosphonate inhibitor[5] and TAM co-crystallized with α,α-difluoro-β-tyrosine[37] or *p*-fluorocinnamate epoxide[38] provided strong evidence for reactions *via N*–MIO intermediates (in which the substrate is connected to MIO through its amino group) for the ammonia-lyase and aminomutase reactions. An alternative covalently bound intermediate was proposed by Rétey[11] and coworkers. In this case, a σ-complex would be formed between the aromatic part of the substrate and the MIO prosthetic group by Friedel-Crafts-like mechanism (FC).

Analysis of the active site residues surrounding the ligand in the L-cysteine-inhibited HAL[5] indicated that the *pro*-(*S*) β-proton from the L-histidine substrate can be abstracted by one of the three residues (Tyr53, Tyr280, Glu414) which might be considered as enzymatic bases (Figure 18). Mutagenesis experiments also demonstrated that Tyr53, Glu414[39] and Tyr280[5,39] are important residues for the catalysis. The remarkably reduced catalytic activity of the analogous tyrosine (Tyr 60 and Tyr300) mutants of TAL implies the importance of Tyr53 and Tyr280 in the HAL reaction.

When PAL was investigated with the phenylalanine analogues D- and L-2-aminooxy-3-phenyl-propionic acid, it was deduced that ammonia elimination approximated the least-motion course.[40] In several *Rs*TAL structures, products of the elimination reaction were found in the active site in a zig-zag orientation.[1] The least-motion course principle and the similar straight chain zig-zag shape of the (*E*)-urocanate product of the HAL reaction determine a straight chain zig-zag arrangement of the covalently bound intermediate and the L-histidine substrate as well. Irrespectively of the nature of the covalently bound reaction intermediate, four reaction paths can fulfill these requirements (Figure **9**).

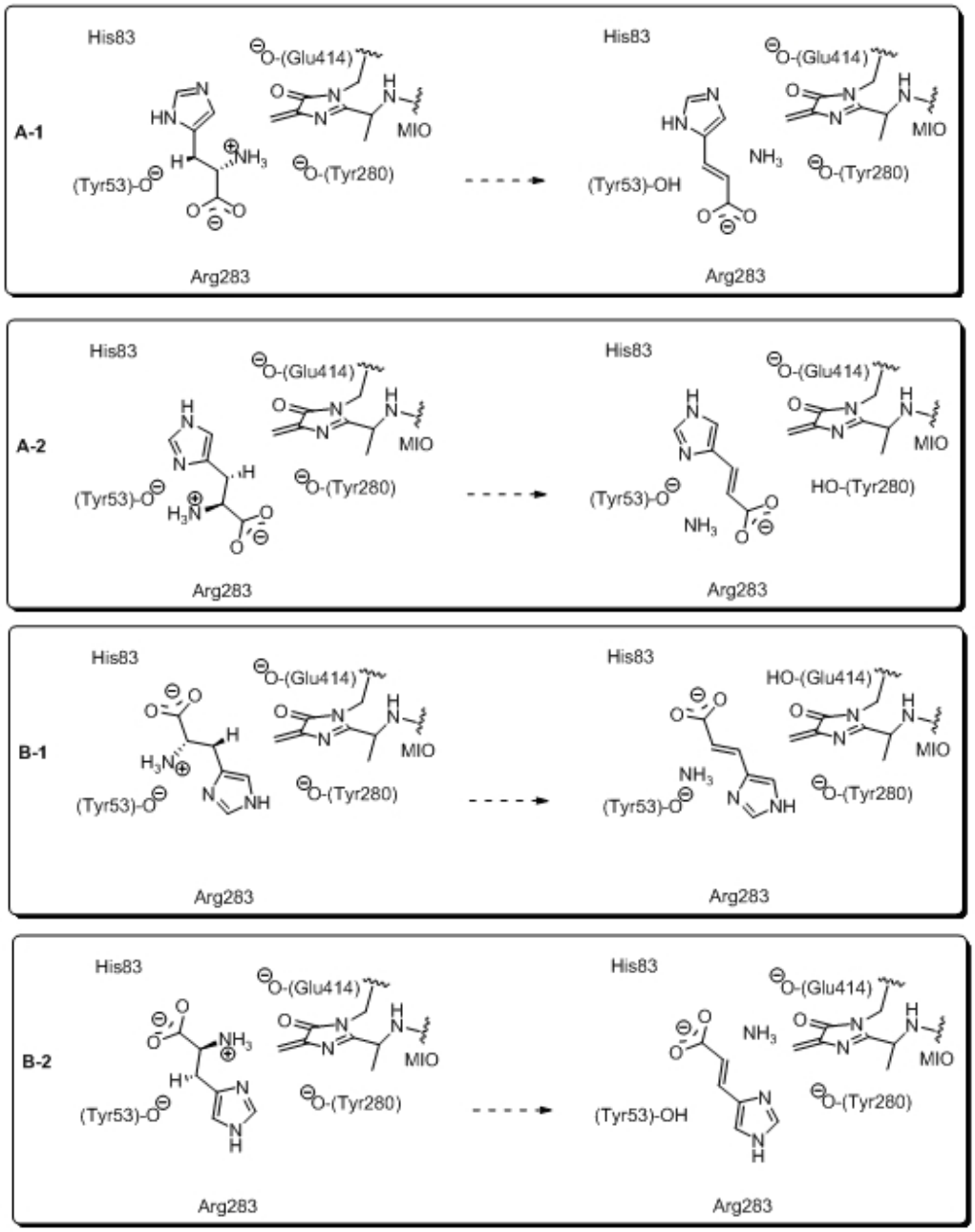

Figure 9. Four possible arrangements of L-histidine and (*E*)-urocanate along the reaction pathways (A-1, A-2, B-1 and B-2) assuming the least-motion course in the HAL active site containing the MIO prosthetic group, His83, Arg283 and three possible enzymatic bases: Tyr53, Tyr280 and Glu414.

Along the **A-1** reaction path for transformation of the substrate to product, both *N*–MIO and FC intermediates are possible but only the Tyr53 amino acid could abstract the *pro*-(*S*) β-proton from the substrate. Only an FC-like mechanism is possible *via* the **A-2** path involving Tyr280 as the base for *pro*-(*S*) β-proton abstraction. Along the **B-1** path, deamination of L-

histidine may take place by the FC mechanism involving Glu414 as an enzymic base. Along the **B-2** path, both types of the mechanism (*N*–MIO and FC) can be taken into account involving Tyr53 as the base for abstraction of the *pro*-(*S*) β-proton.

In addition to the substrate and product states (Figure **9**), the covalently bound reaction intermediate should also fulfill the requirements of least-motion course in the HAL active site. If the HAL reaction proceeded *via* the *N*−MIO intermediate, the amino moiety of the L-histidine substrate would be bound to MIO. If the HAL reaction proceeded *via* a Friedel-Crafts type intermediate, the C_4 carbon of the aromatic ring of L-histidine substrate would form a σ-complex with MIO. However, in this case the reaction may take place *via* two diastereomeric intermediates [(*S,S*)-FC and (*R,S*)-FC] due to a newly forming center of asymmetry at the C_4 carbon of the aromatic ring in the σ-complex.

As in cases of all possible intermediates the substrate was anchored to the enzyme by a covalent bond, the systematic conformational search (CS) with the alternative reaction intermediates was a powerful tool to find their possible arrangements within the HAL active site. Because none of the six HAL[2,5,30] crystal structures indicated significant variations at the most part of the active center, the CSs were performed in rigid enzyme environment. This approach was also supported by the analysis of the B-factors of the active site amino acid residues indicating low mobility (with exception of the residues of the mobile Tyr53-loop).

Because the imidazole ring allowed two different protonation states ($N_{\tau H}$ or $N_{\pi H}$) for each reaction intermediates, six CSs were performed for the three principal alternatives [*N*-MIO-$N_{\tau H}$, *N*-MIO-$N_{\pi H}$, (*R,S*)-FC-$N_{\tau H}$, (*R,S*)-FC-$N_{\pi H}$, (*S,S*)-FC-$N_{\tau H}$, (*S,S*)-FC-$N_{\pi H}$]. Only those conformations were kept which had a straight chain zig-zag arrangement within the lowest 10 kcal/mol range (Table **1**). From the retained conformations of the covalent intermediates of the six CSs, L-histidine and (*E*)-urocanate containing active site models were constructed. The substrate and product and the surrounding eight catalytically relevant amino acid residues were optimized within the closed HAL (1GKM$_{mod}$) active site. In this way, comparative analysis of the full S → I → P(+NH_2) reaction pathways become feasible (Table **1**).

Although the energies obtained at the MM level of theory are usually not accurate enough for reliable enzyme mechanistic studies, several observations are worth mentioning. According to our calculations (Table **1**), energetic results favor the reaction via *N*–MIO ($N_{\tau H}$) type intermediates. In this case, the substrate binding states are of substantially higher energy than the

corresponding reactive *N*–MIO type intermediates and the product binding states are of the lowest energies.

Table 1. MM relative energies of the models of substrate (E_S), intermediate (E_I) and product with MIO-bound amino group (E_{P+NH2}) and the energy difference between the substrate and intermediate states for the two possible protonated forms the three postulated covalent intermediate types. The types of arrangements (according to Fig. 4) for those S → I → P(+NH_2) reaction pathways which satisfy the least-motion principle are shown. Representative H-O distances in the covalent substrate-MIO intermediate structures [I: distances between the ligand's carboxylate-O and the two N-H's of Arg283, and between the *pro*-(*S*) β-hydrogen of the ligand and the O^- atoms of the possible enzymatic bases Tyr53/Tyr280/Glu414;] are also listed. Distances which are shorter than 2.5 Å are emphasized by typing in bold.

	Relative energies (kcal/mol)			Reaction path	H-O distances (Å) in I			
	E_S	E_I	E_{P+NH2}		R283	Y53	Y280	E414
N–MIO ($N_{\tau H}$)								
c1	14.0	7.8	-10.1	A-1	**2.19**/3.12	**2.31**	5.17	6.14
c2	5.6	2.7	-7.5	A-1	3.73/5.20	**2.29**	5.09	5.43
c3	14.0	8.3	-10.7	A-1	**2.19**/3.03	**2.33**	5.23	6.50
c5	13.9	0.2	-10.0	A-1	**2.28**/3.08	**2.36**	5.21	6.45
c8	5.7	0.0	-10.7	A-1	4.37/6.09	**2.37**	5.30	5.64
c9	14.7	7.8	-5.4	B-2	8.41/7.45	**2.13**	4.25	4.83
c11	21.8	15.4	-5.8	A-1	**2.36**/2.89	**2.15**	5.13	6.20
N–MIO ($N_{\pi H}$)								
c1	20.4	11.3	14.9	A-1	4.08/5.36	**2.45**	5.04	5.28
c2	40.4	10.8	0.4	A-1	3.74/5.20	**2.34**	5.12	5.44
c3	24.1	17.9	8.5	A-1	**2.18**/3.12	**2.28**	5.16	6.14
c4	24.0	17.6	6.2	A-1	**2.19**/3.03	**2.31**	5.15	6.24
c6	24.2	19.7	5.5	A-1	**2.19**/2.69	**2.44**	5.12	6.28
c9	31.7	24.1	8.2	A-1	**2.32**/2.85	**2.22**	5.15	6.19
c10	24.9	16.5	5.1	B-2	7.68/8.63	**2.15**	4.13	4.75
(*R,S*)-FC ($N_{\tau H}$)								
c2	30.5	23.1	13.4	B-2	7.64/8.24	4.23	5.40	4.96
c4	28.7	24.0	10.9	B-1	8.79/9.09	4.14	5.43	5.42
c5	26.3	23.1	11.7	B-1	8.24/7.64	4.15	5.39	5.15
c7	28.7	27.2	15.7	B-1	7.41/7.89	2.66	3.18	4.02
c8	25.0	33.1	15.4	B-1	7.97/8.60	4.07	2.63	2.70
c9	28.8	25.9	11.8	B-1	8.99/9.01	3.45	5.84	6.53
(*R,S*)-FC ($N_{\pi H}$)								
c2	25.5	22.8	10.5	B-1	7.63/8.22	4.80	3.71	2.59
(*S,S*)-FC ($N_{\tau H}$)								
c1	27.9	28.6	3.2	B-1	7.34/7.90	2.67	2.92	4.15
c2	25.3	29.0	2.9	B-1	7.87/8.12	2.60	3.00	4.21
(*S,S*)-FC ($N_{\pi H}$)								
c2	27.8	28.5	6.8	B-1	7.53/8.11	2.63	2.92	4.21

Thus, the calculated energy profile of the reaction *via* an *N*–MIO ($N_{\tau H}$) type intermediate is in full agreement with experimental results since MIO-containing ammonia-lyases catalyze, under normal conditions, ammonia elimination from the L-amino acids in a practically irreversible manner.[26,41] All the other intermediate structures had higher energies (10.8-33.1 kcal/mol) than the lowest energy *N*–MIO ($N_{\tau H}$) intermediate conformer.

Next, the H-O distances in the optimized structures of the MIO-bound intermediate models between the ligand's *pro*-(*S*) β-hydrogen and oxygen atoms of the possible enzymic bases (Tyr53, Tyr280 and Glu414) and between ligand's carboxylate oxygen group and Arg283 were analyzed (Table **1**). The most decisive result of this analysis was the observation that there was no enzymic base in any of the FC-intermediate conformations which was close enough to the *pro-(S)* β-hydrogen to abstract it. Therefore, the **A-1** pathway involving an *N*–MIO covalent intermediate is the most plausible for the HAL reaction but a **B-2** type orientation would also be allowed.

The optimized structures containing L-histidine and (*E*)-urocanate ligands in the active site of the closed HAL structure were compared to the arrangements of these ligands obtained by a docking procedure. The analysis of the AutoDock results revealed a well conserved orientation of the product (the carboxylate of the ligand is in the vicinity of the Arg283 while the imidazole moiety points towards His83) and agreed with the results obtained from the MM optimizations. Taking into account the orientation of the product within the active site, the docking results corresponded only to the **A-1** pathway.

3.2.3 The role of Zn(II) in the HAL reaction

It was observed that Zn^{2+} or a number of different divalent cations, like Cd^{2+} or Mn^{2+}, increase the activity of HAL.[42] On the other hand, there is no Zn^{2+} containing crystal structure for HAL.[2,5,30] This apparent contradiction can be resolved by assuming that Zn^{2+}, which is necessary for the catalytic activity, interacts during the HAL reaction with the HAL-specific His83 residue and with the imidazole of the substrate.[39] Therefore, the reason why no Zn^{2+} containing HAL structure is known is that no substrate or product containing HAL structure has been determined so far.[2,5,30] Interaction of a Zn^{2+} with the HAL-specific His83 and with the substrate during the catalysis[39] can also rationalize why HAL accepts only L-histidine,[26] L-4-fluorohistidine[43] or L-4-nitrohistidine[11,44] as substrates.

To examine the contribution of the Zn^{2+} in HAL, model studies were performed on the conformations found for the *N*−MIO intermediate in the $1GKM_{mod}$ active site. Analysis of the existing Zn-containing protein crystal structures[45,46,47,48,49,50] and the calculated *N*−MIO intermediate conformations led to the conclusion that Zn could be coordinated at N_τ atoms of His83 and of the substrate's imidazole (Figure **10a**), similarly as found in Adamalysin II, a zinc endopeptidase from the snake venom of *Crotalus adamanteus*[51] (Figure **10b**).

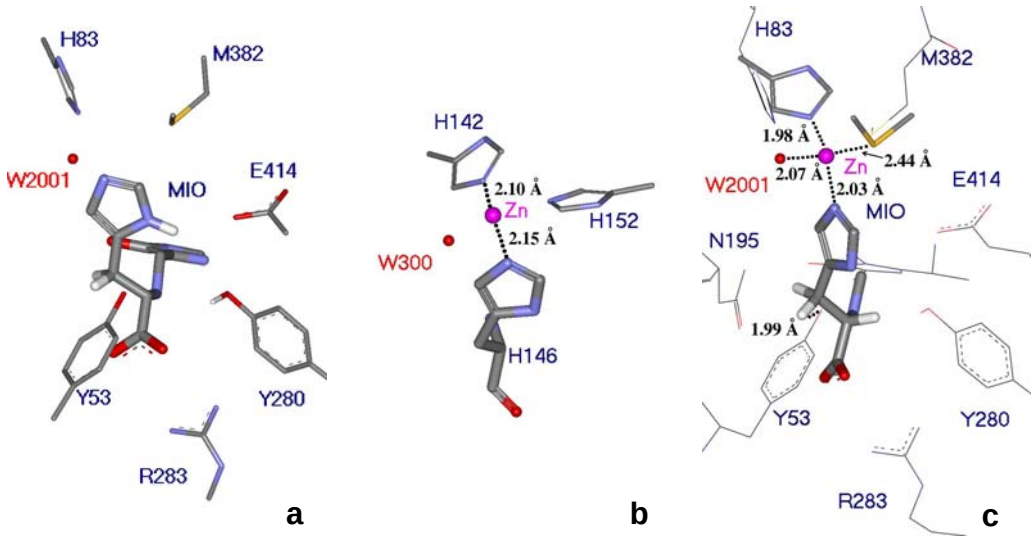

Figure 10 a. Arrangement of the covalent *N*-MIO intermediate ($N_{\pi H}$-c4) in the active site of HAL ($1GKM_{mod}$). **b.** The tetrahedral coordination of Zn (in pink) in the Adamalysin II, a zinc endopeptidase from the snake venom of *Crotalus adamanteus*[51] (PDB code: 1IAG). **c.** Fit of the tetrahedral Zn-complex model (Model 4, by DFT calculation) into the ligand-free active site of HAL ($1GKM_{mod}$).

In the Zn-containing protein structures, two kinds of Zn-complexes can be found.[45,46,47,48,49,50] The Zn may be present in tetrahedral (Th)[45,46,47,48,49,50] or trigonal bypiramidal (Tbp)[45,48] complexes. During the HAL reaction, the further ligands of the Zn^{2+} coordinated to His83 and to the imidazole of L-histidine can be the S atom of the Met382, which is a conserved residue of the histidine ammonia-lyases, and one (in a tetrahedral Zn-coordination, Th) or two water molecules (in a trigonal bipyramidal Zn-coordination, Tbp).

The DFT calculations were performed on the two kinds of truncated Zn-complex structures (Th and Tbp) including all important parts of the active site of HAL (partial elements of MIO, His83, Met382 and one or two conserved water molecules). The DFT calculations indicated that the reaction of HAL should include a tetrahedral Zn-complex, because only tetrahedral complexes resulted in reasonable structures (Table **2**). Optimizations of all possible kinds of

trigonal bipyramidal Zn-complex arrangements aborted or led to tetrahedral structures by exclusion of a water molecule. Comparison of the tetrahedral Zn-complex (Figure **10c**) with the Zn^{2+} complex found in Adamalysin II[51] and with the possible arrangement of the substrate-MIO covalent intermediate obtained by conformational analysis in the Zn-free active site (Figure **10a**) indicated good agreement in the spatial arrangement of the structures.

Table 2 Bond lengths and energies for tetrahedral zinc-ligand complex models calculated by DFT methods.

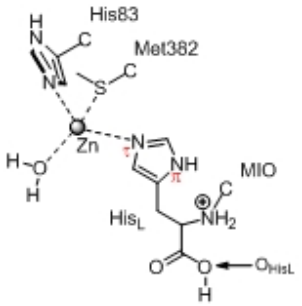

Model	Relative energies (kcal/mol)[a]	Distances (Å)[b]			
		Zn-N_{His83}	Zn-N_{HisL}	Zn-O_{HOH}	Zn-S_{Met382}
1	1.00(0.44)	1.97(1.96)	2.02(2.01)	2.07(2.05)	2.42(2.50)
2	0.00(0.00)	1.96(1.96)	2.03(2.01)	2.06(2.05)	2.42(2.51)
3	2.32(1.57)	1.96(1.96)	2.02(2.01)	2.08(2.05)	2.41(2.49)
4	1.84(0.19)	1.98(1.96)	2.03(2.02)	2.07(2.05)	2.44(2.51)

[a] By single point calculation at QM/QM B3LYP/6-311+G(d,p):B3LYP/6-31G(d) level after optimization of the structures at B3LYP/6-31G(d,p) level; values between brackets are from single point calculations at QM/QM B3LYP/6-311+G(d,p):B3LYP/6-31G(d) level after optimization of the structures at B3LYP/6-31G level. [b] Bond lengths in Zn-complexes optimized at B3LYP/6-31G(d,p) level; values between brackets are for Zn-complexes optimized at B3LYP/6-31G level.

The overlay of the truncated tetrahedral Zn-complex and the ligand-free HAL structure (Figure **10c**) indicated that N_τ atom of the ligand's imidazole was involved in the Zn coordination, whereas the hydrogen atom on the N_π position could be at H-bond distance from Glu414 (Figure **10a** and Figure **10c**). The binding of the ligand during the HAL reaction at its imidazole ring by His83 *via* the Zn-complex and by Glu414 *via* a hydrogen bond is in full agreement with active site mutation data indicating that the Glu414Ala ($k_{cat}/k_{cat\text{-}mut}$= 20930) and the His83Leu ($k_{cat}/k_{cat\text{-}mut}$= 18000) mutations[39] have the most dramatic effect on catalysis. Also, this mode of substrate binding can rationalize the very narrow substrate specificity (in addition to L-histidine, only L-4-fluorohistidine[43] and L-4-nitrohistidine[11,44] are accepted as substrates[26]) of HAL as well.

All the previous results implied that the enzymic base in the HAL reaction which abstracts the *pro*-(*S*) β-hydrogen as a proton is Tyr53. This was indicated by the 1.99 Å distance between

the oxygen atom of Tyr53 and the *pro*-(*S*) β-hydrogen of the tetrahedral Zn-complex as well (Figure **10c**). To estimate the acidity of the *pro*-(*S*) β-hydrogen in the conformations allowed in the closed active site of HAL, analysis of Mülliken charges of hydrogens at the β-position of L-histidine, L-4-nitrohistidine and truncated models for the Zn-free and Zn-coordinating *N*–MIO intermediates was performed (Table **3**). Because it is known that the nitro group acidifies the *pro*-(*S*) β-hydrogen of L-4-nitrohistidine[44] and it is accepted as substrate even by the MIO-less mutant of HAL analysis of L-4-nitrohistidine was also included.

Table 3 Mülliken atomic charges of the *pro*-(*S*) β-hydrogens in zwitterionic L-histidine, in zwitterionic L-4-nitrohistidine, in a truncated *N*-MIO-intermediate model and in the tetrahedral Zn-complex models.

Entry	Structure[a]	H_S	H_R
1	*N*-MIO (truncated model)	0.176 (0.221)	0.133 (0.173)
2	L-Histidine	0.180 (0.222)	0.102 (0.166)
3	L-4-Nitrohistidine	0.199 (0.245)	0.135 (0.201)
4	Zn-complex, Model 1	0.220(0.267)	0.172 (0.206)
5	Zn-complex, Model 2	0.220 (0.265)	0.173 (0.208)
6	Zn-complex, Model 3	0.220 (0.263)	0.174 (0.208)
7	Zn-complex, Model 4	0.215 (0.261)	0.177 (0.210)

[a] Calculations on the ligand conformations allowed within the HAL active site were performed at B3LYP/6-31G(d,p) level (values between brackets are from B3LYP/6-31G DFT calculations).

The Mülliken charges found for *pro*-(*S*) β-hydrogen at the optimized geometries of L-histidine, L-4-nitrohistidine ($N_{\tau H}$ forms) and the Zn-complex models (Table **3**) indicated that the acidity of the *pro*-(*S*) β-hydrogen was significantly higher in L-4-nitrohistidine (Entry 3) than in the L-histidine (Entry 2) or in the Zn-free *N*–MIO model (Entry 1). The most charged *pro*-(*S*) β-hydrogens, however, were found in the Zn-complex models (Entries 4-7).

These results imply that the formation of a transient Zn-complex in the HAL reaction contributes not only to the specific binding of the substrate but to the enhancement of its reactivity as well.

Conclusions

I. The modified, closed PAL structure (constructed by modeling the 83-141, 321-351 loops with the catalytically essential Tyr53 on the basis of *Rs*TAL) resulted less deviations from the allowed side chain conformations in the Ramachandran-plot than the original experimental structure.

II. The presented ligand docking and conformational analysis results of the covalently bounded L-phenylalanine to the MIO prosthetic group of the PAL reaction within an essential portion of the *Petroselinum crispum* phenylalanine ammonia-lyase (*Pc*PAL) including the full, tightly closed active center support the idea that the PAL reaction proceeds *via* the *N*-MIO intermediate state in which the L-phenylalanine ligand is covalently bound to the MIO prosthetic group through its N-atom (*N*-MIO).

III. The existing crystal structures for HAL, PAL, TAL, and sequence comparison of the active site residues for all the known MIO-containing enzymes indicate that besides the electrophilic MIO prosthetic group, these two Tyr, the Arg, the two Asn residues (except for HAL, in which one Asn is different) belong to the arrangement train of the known MIO-enzymes.

IV. The new partially modified TAL based 1B8F$_{mod}$ HAL structure is a more competent reliable model. This HAL model revealed that the catalytically important amino acid (Tyr53) is located at highly isosteric position in the active site. The new *Pp*HAL structure can be considered as more accurate model of the active state of the enzyme than the existing experimental HAL structures.

V. The present study revealed also that the existing experimental structures of histidine ammonia-lyase from *Pseudomonas putida* (*Pp*HAL) contain an essential Tyr53-containing loop in a partially opened conformation. The modified, closed 1GKM$_{mod}$ HAL structure (constructed by modeling the 39-80 loop with the catalytically essential Tyr53 on the basis of *Av*PAL) resulted less deviations from the allowed side chain conformations in the Ramachandran-plot than the original experimental structure.

VI. Investigation of distances between the acidic *pro*-(*S*) β-hydrogen at C_2 of ligand and the appropriate oxygen atoms of the possible enzymic bases Tyr53, Ty280 and Glu414 in the calculated conformations of the three proposed structures [*N*−MIO, (*R,S*)-FC, (*S,S*)-FC] of the covalently bound reaction intermediate within the closed active site of HAL revealed that the reaction can only take place *via* the *N*−MIO intermediate structure which allowed Tyr53 to get close enough to the *pro*-(*S*) β-hydrogen. This conclusion was also supported by the docking results with (*E*)-urocanate.

VII. DFT calculations on the role of a Zn^{2+} ion in the HAL reaction using a truncated model of the *N*−MIO intermediate indicated the formation of a tetrahedral complex with a Zn^{2+} ion coordinated to the imidazole ring of the ligand, to His83 and Met382 residues of the enzyme and to a water molecule. The formation of such transient Zn-complex could explain the narrow substrate specificity of HAL. The DFT calculations indicated also that the formation of a Zn-complex had a contribution to the enhancement of the *pro*-(*S*) β-hydrogen's reactivity in the *N*−MIO intermediate as well.

VIII. The good match of predicted and experimental structures gave confidence that the docking method is able to provide relevant information about the substrate/product interaction with the enzyme, but the results of the geometry optimizations of L-histidine/(E)-urocanic acid meet the requirements of the experimental data found for ligands within the X-ray structure of other ammonia-lyases. The same interactions appear in the case of the L-histidine substrate together with other interaction that one between its amino moiety and methylene part of MIO group.

List of Publications

Publications on the PhD subject

Papers

1. **Seff A.L.**, Pilbák S., Silaghi-Dumitrescu I.†, Poppe L., Computational Investigation of the Histidine Ammonia-Lyase Reaction: a Modified Loop Conformation and the Role of the Zinc(II) Ion, *Journal of Molecular Modeling*, **2010**, *submitted*.
2. **Seff A.L.**, Pilbák S., Silaghi-Dumitrescu I.†, Poppe L., Computational Investigation of a Bacterial Histidine Ammonia-Lyase (HAL) Model with a Completely Closed Active Center, *Studia Universitatis Babes-Bolyai, Seria Chemia*, **2010**, XLV, *2*, TOM I, *p. 37-45*.
3. **Seff A.L.**, Pilbák S., Poppe L., Ligand Docking and Systematic Conformational Analysis in Loop Modified *Parsley* Phenylalanine Ammonia-Lyase Structure, *Studia Universitatis Babes-Bolyai, Seria Chemia*, **2008**, LIII, 2, *p 67-71*.
4. **Seff A.L.**, Pilbák S., Silaghi-Dumitrescu I.†, Poppe L., Ligand Docking and Systematic Conformational Analysis in Loop Modified Phenylalanine Ammonia-Lyase Structure, *XIIIth International Chemistry Conference*, Hungarian Technical Scientific Society from Transylvania, Cluj-Napoca, Romania, November 8-11, **2007**, ISSN 1843-6293, Book of Works, *p 106-109.*

Oral presentations

5. **Seff A.L.**, Pilbák S., Poppe L., Silaghi-Dumitrescu I.†, DFT Studies on the Formation of an Intermediate Tetrahedral Zn^{2+} Complex in a Closed Active Center of HAL, *Molecular Modeling in Chemistry and Biochemistry MOLMOD*, Special Edition, Cluj-Napoca, Romania, **Plenary Lecture**, May 28, **2010**.
6. **Seff A.L.,** Pilbák S., Silaghi-Dumitrescu I.†, Poppe L., Zinc-Containing Active Site in a Partially Modified 1GKM Crystal Structure of Histidine Ammonia-Lyase: A Computational Investigation., *Molecular Modeling in Chemistry and Biochemistry MOLMOD*, Cluj-Napoca, Romania, **Plenary Lecture**, April 2-4, **2009**, Book of Abstracts, *p 17*.
7. **Seff A.L.**, Pilbák S., Silaghi-Dumitrescu I.†, Poppe L., Ligand Docking and Systematic Conformational Analysis in Loop Modified Phenylalanine Ammonia-Lyase Structure, *XIIIth International Chemistry Conference*, Hungarian Technical Scientific Society from Transylvania, Cluj-Napoca, Romania, **Plenary Lecture**, November 8-11, **2007**, ISSN 1843-6293, Book of Works, *p 106-109*.
8. **Seff A.L.**, Pilbák S., Poppe L., Ligand Docking and Systematic Conformational Analysis in Loop Modified Parsley Phenylalanine Ammonia-Lyase Structure, *Molecular Modeling in Chemistry and Biochemistry MOLMOD*, Arcalia, Romania, **Plenary Lecture**, July 5-8, **2007**, ISBN 978-973-7973-46-7, Book of Abstracts, *p 15*.

Posters

9. **Seff A.L.**, Pilbák S., Silaghi-Dumitrescu I.†, Poppe L., Computational Investigation of a Bacterial Histidine Ammonia-Lyase (HAL) Model with a Completely Closed Active Center, *4th Central European Conference: Chemistry towards Biology*, Dobogókő, Hungary, **poster,** September 8-11, **2008**, Book of Abstracts, *p124*.

10. **Seff A.L.**, Pilbák S., Silaghi-Dumitrescu I.†, Poppe L., A new Bacterial Histidine Ammonia-Lyase (HAL) Model with a Completely Closed Active Center Investigated by Computation, *23rd International Conference on Organometallic Chemistry*, Rennes, France, **poster**, July 13-18, **2008**, Book of Abstracts, *P473*.
11. **Seff A.L.**, Pilbák S., Silaghi-Dumitrescu I.†, Poppe L., Comparison of Ligand Docking and Conformational Analysis Results in Loop Modified Parsley Phenylalanine Ammonia-Lyase Structure, *Homboldt Conference on Noncovalent Interactions*, Vrsac, Serbia, **poster**, November 15-18, **2007**, Book of Abstract, *p 40-41*.

Other publications

12. **Seff A.L.**, Darvasi J., Kékedy-Nagy L., Borszéki J., Halmos P., Determination of Element Containing in Chicken Bone and Comparison of Different Decomposition Methods*,* XIth International Chemistry Conference, Hungarian Technical Scientific Society from Transylvania, Cluj-Napoca, Romania, **Plenary Lecture,** November 11-13, **2005**, **MKE** (Society of Hungarian Chemists) **prize**, ISBN 973-7840-07-0, Book of Works, *p 55-58*.
13. **Seff A.L.**, Darvasi J., Comparisons of Decomposition and Determination Methods for Quantification of Some Heavy Metal from Domestic Birds Bones, *Students for students" Session of Scientific Student Communication*, 2nd Edition, Cluj-Napoca, Romania, **Oral Presentation**, April 8-10, **2005**, Book of Abstracts, *p. 72*.
14. **Seff A.L.**, Darvasi J., Analysis of Metatarsus Bones of Fowls, *Scientific National Conference for Students, Chemistry Section*, XXVIIth Edition, Budapest, Hungary, **Oral Presentation**, March 23, **2005**, **Honorable mention**, Work of 30 pages.
15. **Seff A.L.**, Darvasi J., Determination by ICP of Heavy Metals Containing in Metatarsus Chicken Bone Samples Decomposited with Open- and Closed Type Microwave Oven, *Scientific Conference for Students in Spring 2004, Chemistry Section*, Szeged, Hungary, **Oral Presentation**, April 29-30, **2004**, **Honorable mention**, Work of 29 pages.
16. **Seff A.L.**, Silaghi-Dumitrescu I.†, Calcule DFT asupra interacţiunii acizilor Lewis EX4 din grupa 14 cu baze Lewis, *XXIXth National Chemistry Conference*, Călimăneşti-Căciulata, Vâlcea, Romania, **poster**, October 4-6, **2006**, Book of Abstracts, *P.S.II. – 41*.

Selected references

[1] Louie G.V., Bowman M.E., Moffitt M.C., Baiga T.J., Moore B.S., Noel J.P., *Chemistry and Biology*, **2006**, *13*, 1327-1338.
[2] Schwede T.F., Rétey J., Schulz, G.E., *Biochemistry*, **1999**, *38*, 5355-5361.
[3] Ritter H., Schulz G.E., *Plant Cell*, **2004**, *16*, 3426-3436.
[4] Calabrese J.C., Jordan D.B., Boodhoo A., Sariaslani S., Vanneli T., *Biochemistry*, **2004**, *43*, 11403-11416.
[5] Baedeker M., Schulz G.E., *European Journal of Biochemistry*, **2002**, *269*, 1790-1797.
[6] Poppe L., *Current Opinion in Chemical Biology*, **2001**, *5*, 512-524.
[7] Rétey J., *Biochimica et Biophysica Acta*, **2003**, *1647*, 179-184.
[8] Wang L., Gamez A., Archer H., Abola E.E., Sarkissian C.N., Fitzpatrick P., Wendt D., Zhang J., Vellard M., Bliesath J., Bell S.M., Lemontt J.F., Scriver C.R., Stevens R.C., *Journal of Molecular Biology*, **2008**, *380*, 623-635.
[9] Hanson K.R., Havir E.A., *Archives of Biochemistry and Biophysics*, **1970**, *141*, 1-17.
[10] Hermes J.D., Weiss P.M., Cleland W.W., *Biochemistry*, **1985**, *24*, 2959-2967.
[11] Langer M., Pauling A., Rétey J., *Angewandte Chemie International Edition*, **1995**, *34*, 1464-1465.
[12] Swiss-Model, An automated Comparative Protein Modelling Server, http://swissmodel.expasy.org/
[13] Arnold K., Bordoli L., Kopp J., Schwede T., *Bioinformatics*, **2006**, *22*,195-201.
[14] Kopp J., Schwede T., *Nucleic Acids Research*, **2004**, *32*, D230-D234.
[15] Schwede T., Kopp J., Guex N., Peitsch M.C., *Nucleic Acids Research*, **2003**, *31*, 3381-3385.
[16] Guex, N., Peitsch M.C., *Electrophoresis*, **1997**, *18*, 2714-2723.
[17] Peitsch M.C., Bio/Technology, 1995, 13, 658-660.
[18] Hyperchem version 7.0 (Hypercube, Inc. http://www.hyper.com/).
[19] Arguslab program (http://www.arguslab.com).
[20] Frisch M.J., Trucks G.W., Schlegel H.B., Scuseria G.E., Robb M.A., Cheeseman J.R., Scalmani G., Barone V., Mennucci B., Petersson G.A., Nakatsuji H., Caricato M., Li X., Hratchian H.P., Izmaylov A.F., Bloino J., Zheng G., Sonnenberg J.L., Hada M., Ehara M., Toyota K., Fukuda R., Hasegawa J., Ishida M., Nakajima T., Honda Y., Kitao O., Nakai H., Vreven T., Montgomery Jr. J.A., Peralta J.E., Ogliaro F., Bearpark M., Heyd J.J., Brothers E., Kudin K.N., Staroverov V.N., Kobayashi R., Normand J., Raghavachari K., Rendell A., Burant J.C., Iyengar S.S., Tomasi J., Cossi M., Rega N., Millam N.J., Klene M., Knox J.E., Cross J.B., Bakken V., Adamo C., Jaramillo J., Gomperts R., Stratmann R.E., Yazyev O., Austin A.J., Cammi R., Pomelli C., Ochterski J.W., Martin R.L., Morokuma K., Zakrzewski V.G., Voth G.A., Salvador P., Dannenberg J.J., Dapprich S., Daniels A.D., Farkas Ö., Foresman J.B., Ortiz J.V., Cioslowski J., Fox D.J., *Gaussian 09, Revision A.1.* **2009**, Gaussian, Inc., Wallingford CT.
[21] Dennington II Roy, Keith Todd, Millam John, Eppinnett Ken, Hovell W. Lee, and Gilliland Ray, *GaussView, Version 3.09*, **2003**, Semichem, Inc., Shawnee Mission, KS.
[22] Becke A.D., *Journal of Chemical Physics*, **1993**, *98*, 5648-5652.
[23] Lee C., Yang W., Parr R.G., *Physical Review B*, **1988**, *37*, 785-789.
[24] Pilbák S., Tomin A., Rétey J., Poppe L., *The FEBS Journal*, **2006**, *273*, 1004-1019.
[25] Seff A.L., Pilbák S., Poppe L., *Studia Universitatis Babes-Bolyai, Seria Chemia*, **2008**, LIII, *2*, 67-71.

[26] Poppe L., Rétey J., *Angewandte Chemie, International Edition English*, **2005**, *44*, 3668-3688.
[27] Morrison H., Bernasconi C., Pandey G., *Photochemistry and Photobiology*, **1984**, *40*, 549-550.
[28] Taylor R.G., Levy H.L., McInnes R.R., *Molecular Biology and Medicine*, **1991**, *8*, 101-116.
[29] Seff A.L., Pilbák S., Silaghi-Dumitrescu I., Poppe L., *4th Central European Conference: Chemistry towards Biology*, September 8-11, **2008**, Book of Abstracts, Dobogókő, Hungary, p124.
[30] Baedeker M., Schulz G.E., *Structure*, **2002**, *10*, 61-67.
[31] Moffitt M.C., Louie G.V., Bowman M.E., Pence J., Noel J.P., Moore B.S., *Biochemistry*, **2007**, *46*, 1004-1012.
[32] Klee C.B., *Biochemistry*, **1974**, *13*, 4501-4507.
[33] Hernandez D., Stroh J.G., Phillips A.T., *Archives of Biochemistry and Biophysics*, **1993**, *307*, 126-132.
[34] Merkel D., Rétey J., *Helvetica Chimica Acta*, **2000**, *83*, 1151-1160.
[35] Galpin D., Ellis, B.E., Tanner, M.E., *Journal of American Chemical Society*, **1999**, *121*, 10840-10841.
[36] Peterkofsky A., *Journal of Biological Chemistry*, **1962**, *237*, 787-795.
[37] Christianson C.V., Montavon T.J., Festin G.M., Cooke H.A., Shen B., Bruner S.D., *Journal of American Chemical Society*, **2007**, *129*, 15744-15745.
[38] Montavon T.J., Christianson C.V., Festin G.M., Shen B., Bruner S.D., *Bioorganic and Medicinal Chemistry Letters,* **2008**, *18*, 3099-3102.
[39] Röther D., Poppe L., Viergutz S., Langer B., Rétey J., *European Journal of Biochemistry*, **2001**, *268*, 6011-6019.
[40] Hanson K.R., *Archives of Biochemistry and Biophysics*, **1981**, *211*, 575-588.
[41] Rétey J., *Biochimica et Biophysica Acta*, **2003**, *1647*, 179-184.
[42] Klee C.B., *The Journal of Biological Chemistry*, **1972**, *247*, 1398-1406.
[43] Klee C.B., Kirk K.L., Cohen L.A., McPhie P., *Journal of Biological Chemistry*, **1975**, *250*, 5033-5040.
[44] Klee C.B., Kirk K.L., Cohen L.A., *Biochemical and Biophysiscal Research Communications*, **1979**, *87*, 343-348.
[45] Nauton L., Kahn R., Garau G., Hernandez J.F., Dideberg O., *Journal of Molecular Biology*, **2008**, *375*, 257-269.
[46] Bebrone C., *Biochemical Pharmacology*, **2007**, *74*, 1686-1701.
[47] Martini D., Ranieri-Raggi M., Sabbatini A.R.M., Moir A.J.G., Polizzi E., Mangani S., Raggi A., *Biochimica et Biophysica Acta*, **2007**, *1774*, 1508-1518.
[48] Lipscomb W.S., Strater N., *Chemical Reviews*, **1996**, *96*, 2375-2433.
[49] Gerhardt S., Hassal G., Hawtin P., McCall E., Flavell E., et al., *Journal of Molecular Biology*, **2007**, *373*, 891-902.
[50] Debela M., Goettic P., Magdolen V., Huber R., Schechter N.M., Bode W., *Journal of Molecular Biology*, **2007**, *373*, 1017-1031.
[51] Gomis-Rüth F.X., Kress L.F., Bode W., *EMBO Journal*, **1993**, *12*, 4151-4157.